

## Application of Pseudorandom m-Sequences for Seismic Acquisition

Joe Wong\*  
University of Calgary, Calgary, AB, Canada  
wongjoe@ucalgary.ca

### Maximal-Length Sequence PRBS

Maximal-length sequences (or m-sequences) are well-defined mathematical constructs with impulse-like autocorrelations that make them attractive for use in seismic acquisition. They are easily produced by logic statements in software, or they can be generated electronically by simple circuits with shift registers and gates connected in specific feedback loops (Golomb, 1967). A particular m-sequence is a periodic stream of 1's and -1's characterized by its sequence length  $L$  and base period  $\tau$ . The sequence length  $L$  is given by

$$L = (2^m - 1), \quad (1)$$

where  $m$  is a positive integer called the degree of the sequence. Sequences of lengths 31, 127, 2047, and 32767 are defined when  $m$  assumes the values 5, 7, 11, and 15. The base period  $\tau$  is the shortest time between adjacent transitions in the sequence, and  $T = L \cdot \tau$  is the period of the sequence. Because an m-sequence is periodic, its power spectrum discrete; with values at the discrete frequencies  $f_n = n \cdot \Delta f$  being defined by the sinc-squared function:

$$S_L(n \cdot \Delta f) = \sin^2(\pi \cdot n / L) / (\pi \cdot n / L)^2, \quad n = 0, 1, 2, \dots, L, L+1, L+2, \dots \quad (2)$$

$$\Delta f = 1 / (L \cdot \tau) .$$

Equations 1 and 2 show that sequence period  $T$  and the power spectrum can be adjusted by changing the parameters  $m$  and  $\tau$ . Figure 1a is an m-sequence with  $L=31$ ,  $\tau=4.0$  milliseconds, and  $T=124$ msec. Its autocorrelation, shown in Figure 1b, is periodic, with well-defined triangular shapes that peak at times equal to  $n \cdot L \cdot \tau$ . The base widths of the triangles are 8msec, or  $2 \cdot \tau$ . If we scale the autocorrelation so that the peaks have the value  $L$  (in this case, 31), then the autocorrelation peaks will rest on a perfectly flat DC value of -1. The ratio of the correlation peak value to the DC value will equal  $(-L)$  for any m-sequence.

Figure 1c is an m-sequence with  $L=127$ ,  $\tau=1$ msec, and period  $T = 127$ msec. We see in Figure 1d that its autocorrelation peaks are much sharper than those seen in Figure 1b. The scaled peak and DC values are 127 and -1, respectively, while the base widths of the triangular peaks are 2msec. If we keep increasing the value of  $L$  by increasing  $m$  in Equation 1, while decreasing  $\tau$  (by a factor of 2 each time  $m$  changes by 1 so as to keep the sequence period  $T$  almost constant), the correlation peak becomes a better and better approximation to the delta function.

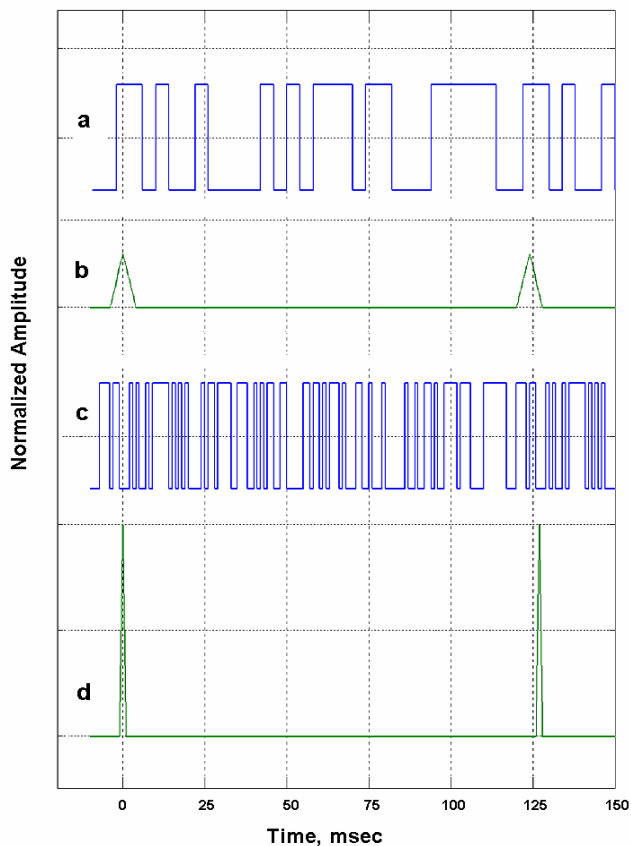


Fig. 1 (a) m-sequence with  $L=31$ ,  $\tau=4.0$  msec.; (b) autocorrelation of Figure 1a; (c) m-sequence with  $L=127$  and  $\tau=1.0$  msec; (d) autocorrelation of Figure 1c.

A defining characteristic of a perfectly random signal or pure noise is that its autocorrelation is a delta function. The autocorrelation of an m-sequence makes it clear why it is considered to be a pseudorandom signal. The sharp triangular peaks become narrower in absolute time as  $\tau$  is made smaller, and the peak values relative to the DC base level become larger as the sequence length  $L$  increases. Longer and longer m-sequences behave more and more like a true noise signal. M-sequences have only two values, +1 and -1, so they are often referred to as pseudorandom binary sequences, or PRBS.

The special characteristics of m-sequences have prompted numerous researchers to use them for analyzing linear systems (Engelberger and Benjamin, 2005). They have been incorporated into long-range radar and sonar applications where signal-to-noise enhancement is critical.

For example, the earliest experiments in detecting radar echoes from Venus employed PRBS technology (Price et al., 1959). Behringer et al. (1982) and Dushaw et al. (1999) studied fluctuations in seawater acoustic velocities across thousands of kilometers using PRBS-coded sonar signals. Sachs et al. (2003) have described how modern short-range radar systems have adopted PRBS coding. Duncan et al. (1981) employed PRBS signals in a controlled source audiofrequency magnetotelluric (CSAMT) experiment.

### Seismic Acquisition Using PRBS Crosscorrelation

Figure 2 shows the basic principles of using a PRBS in seismic data acquisition. A PRBS with fundamental length  $L=127$ , base period  $\tau=1$ msec has been digitized with a sampling time of 0.25msec and plotted in Fig 2a. The sequence is delayed by 40msec and shown on Figure 2b

(the PRBS is periodic, so that, in being delayed, its end wraps around to the beginning). The delayed sequence is crosscorrelated with the original sequence, and the shifted correlation peaks, shown on Figure 2c, confirm that the delay is 40msec. Figure 2d is a seismic wavelet representing the impulse response of a seismic source. When the seismic source is driven by the undelayed PRBS, it generates a signature which is the convolution of the PRBS and the seismic wavelet. This signal propagates through the earth and is detected by a sensor some distance away. The detected signal is represented by Figure 2e, which is the convolution of the PRBS and the wavelet, delayed by the travel time. Figure 2f is the crosscorrelation of the delayed convolution with the undelayed PRBS, showing the recovered wavelet arriving at the proper delay time.

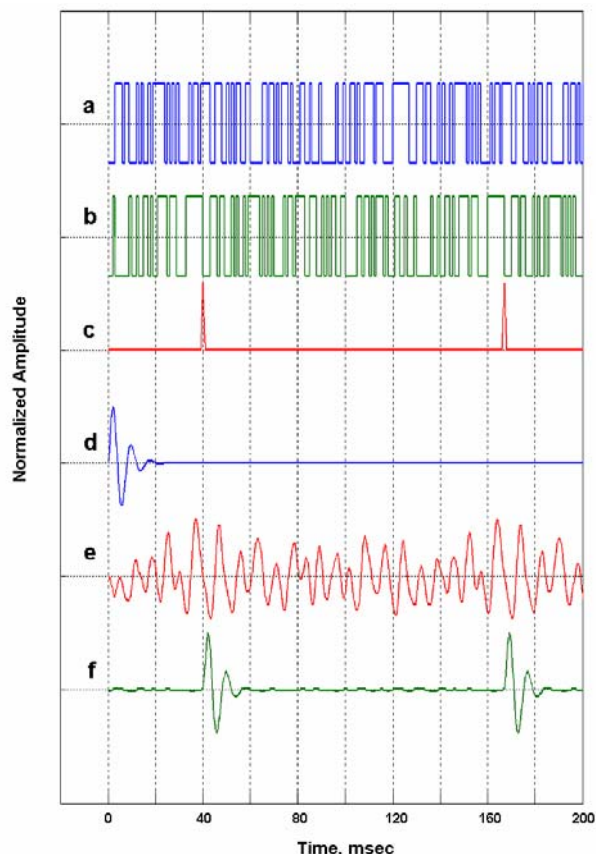


Fig. 2 (a) PRBS with  $L=127$ ,  $\tau=1.0$  msec; (b) PRBS delayed by 40 msec; (c) crosscorrelation of delayed PRBS with original PRBS; (d) a seismic wavelet; (e) wavelet convolved with delayed PRBS; (f) crosscorrelation of convolution 2e with undelayed PRBS.

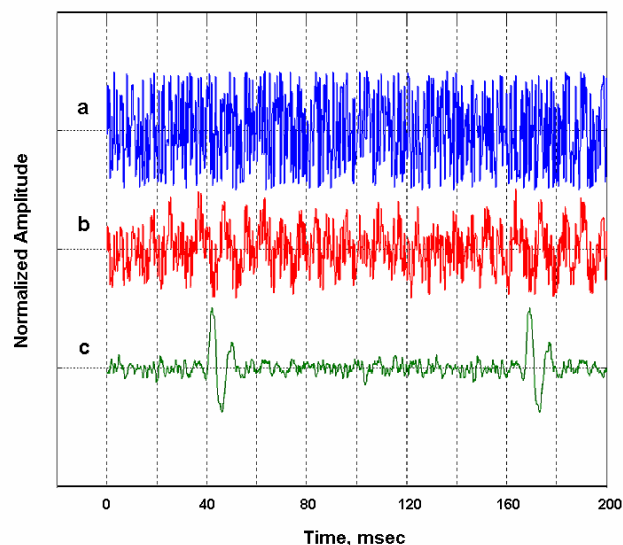


Fig.3 (a) The seismic wavelet in Figure 2d, plus random noise; the wavelet is completely obscured; (b) the seismic wavelet convolved with the delayed PRBS, plus the same random noise; (c) crosscorrelation of the noisy convolution with the undelayed PRBS of Figure 2a, recovering the delayed wavelet with much improved signal-to-noise ratio.

## Noise Rejection Capabilities

The ability of PRBS crosscorrelation to pull weak signals out of strong random noise is its most important and useful property. Figure 3a is the seismic wavelet in Figure 2d with random background noise added. The signal-to-noise ratio (SNR), as determined by the amplitude of the wavelet and the mean noise amplitude, is about 1. The wavelet is completely obscured by the noise. Figure 3b is the delayed convolution of Figure 2e plus the same random noise. The SNR is somewhat higher, but it is still difficult to discern any signal. However, when we crosscorrelate Figure 3b with the original PRBS (Figure 2a), we recover the seismic arrival very effectively (Figure 3c).

In Figure 4, the signal amplitude is decreased to about 20% of the noise level. As the convolution/crosscorrelation method is applied using longer and longer sequences, the signal emerges more and more clearly above the noise. In principle, PRBS crosscorrelation will enhance signal power over random noise power by a factor equal to the sequence length  $L$ .

### Seismograms Acquired with PRBS Correlation

High-resolution seismic imaging of oil and gas reservoirs may require wavelengths on the order of several meters to several tens of meters. In typical reservoir rocks, the frequencies must be in the range 200 to 2000 Hz (Harris et al., 1995; Fogues et al., 2006). Such frequencies can be produced easily by using piezoelectric materials as transducers.

However, the output power of piezoelectric sources is low, and techniques for signal-to-noise enhancement must be employed to obtain good seismograms across useful distances. To this end, Harris et al. (1995) and Fogues et al. (2006) used crosscorrelation and frequency sweeps with their piezoelectric sources. Alternatively, Wong et al. (1983), Yamamoto et al. (1994), and Wong (2000) chose crosscorrelation with m-sequences for their piezoelectric vibrators.

Figure 5 shows seismograms acquired through igneous rock using a piezoelectric vibrator with PRBS coding. The gather was recorded in a crosswell configuration with hydrophones in a well about 80 meters from the source well. The dominant frequencies in these seismograms are about 3.3 kHz. The sample time is .05msec.

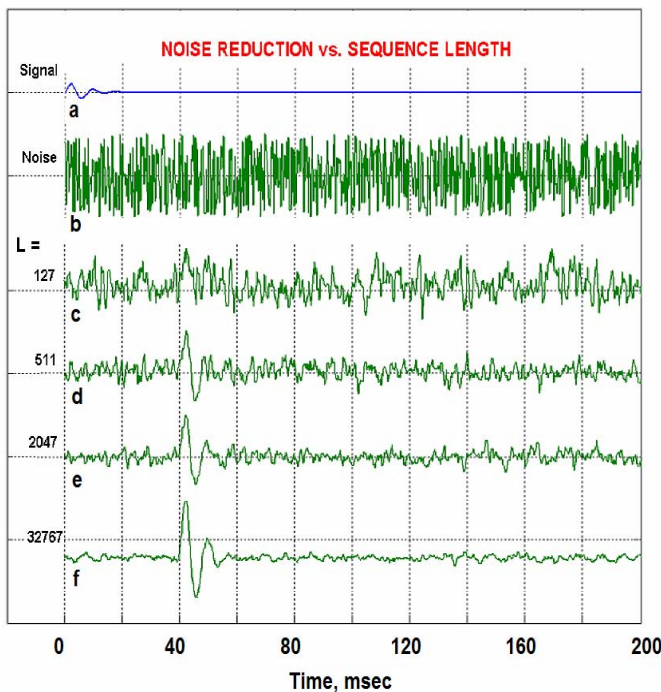


Fig. 4 (a) A small-amplitude signal; (b) random noise, with amplitude five times the signal amplitude; (c), (d), (e), and (f) noise reduction as in Figure 3, using m-sequences with  $L = 127, 511, 2047,$  and  $32767$ .

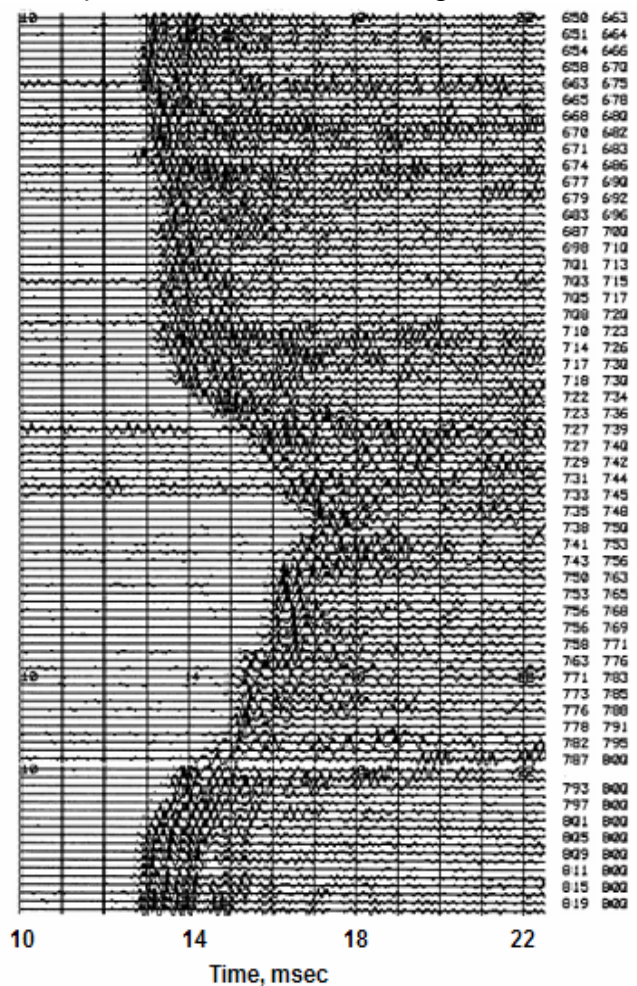


Fig. 5. Crosswell seismograms acquired with PRBS cross-correlation. Sequence parameters:  $L=2047$ ;  $\tau = 0.10$ msec. Source and receiver depths in meters in columns at right.

## References

- Behringer, D., Birdsall, T., Brown, M., Cornuelle, B., Heinmiller, R., Knox, R., Metzger, K., Munk, W., Speisberger, J., Spindel, R., Webb, D., Worcester, P., Wunsch, C., 1982, A demonstration of ocean acoustic tomography: *Nature*, **299**, 121-125.
- Duncan, P.M., Hwang, A., Edwards, R.N., Bailey, R.C., and G.D. Garland, 1980, The development and applications of a wide band electromagnetic sounding system using a pseudo-noise source, *Geophysics*, **45**, 1276-1296.
- Dushaw, B.D., Howe, B.M., Mercer, J.A., and Spindel, R.C., 1999, Multimegahertz-range acoustic data obtained by bottom mounted hydrophone arrays for measurement of ocean temperature: *IEEE J. of Ocean Engineering*, **24**, 202-214.
- Engelberger, S., and Benjamin, H., 2005, Pseudo-random sequences and the measurement of the frequency response: *IEEE Instrumentation and Measurement Magazine*, **8**, 54-59.
- Fogues, E., Meunier, J., Gresillon, F.X., Hubans, C., and Druesne, D., 2006, Continuous high-resolution seismic monitoring of SAGD: 76<sup>th</sup> Ann. Internat. Mtg., SEG, Expanded Abstracts, TL2.4, 3165-3169.
- Golomb, S., 1967, Shift register sequences: Holden-Day, San Francisco.
- Harris, J.M., Nolen-Hoeksema, R.C., Langan, R.T., Van Schaak, M., Lazaratos, S.K., and Rector, J.W., 1995, High-resolution crosswell imaging of a west Texas carbonate reservoir: Part I-Project summary /interpretation: *Geophysics*, **60**, 667-681.
- Price, R., Green, P.E., Goblick, P.J., Kingston, R.H., Kraft, L.G., Pettengill, G.H., Silver, R., and Smith, W.B., 1959, Radar echoes from Venus: *Science*, **129**, 751-753.
- Sachs, J., Zetick, R., Peyerl, P., and Raushenbach, P., 2003, M-sequence ultra-wideband radar, state of development and applications: *Proc. RADAR*, Sept. 2-3, 2003, Adelaide, Australia.
- Wong, J., Hurley, P., and West, G.F., 1983, Crosshole seismology in crystalline rocks: *Geophys. Res. Lett.*, **10**, 686-689.
- Wong, J., 2005, Crosshole seismic imaging for sulfide orebody delineation near Sudbury, Ontario: *Geophysics*, **65**, 1900-1907.
- Yamamoto, T., Nye, T., Kuru, M., 1994, Porosity, permeability, shear strength: crosswell tomography beneath an iron foundry: *Geophysics*, **59**, 1530-1541.